Int. J. Heat Mass Transfer. Vol. 27, No. 4, pp. 553–560, 1984
Printed in Great Britain

0017–9310/84 $3.00 + 0.00

ANALYSIS OF LAMINAR FLOW AND HEAT TRANSFER IN TUBES WITH INTERNAL CIRCUMFERENTIAL FINS

G. J. ROWLEY† and S. V. PATANKAR
Department of Mechanical Engineering, University of Minnesota, Minneapolis, MN 55455, U.S.A.

(*Received* 31 *January* 1983 *and in revised form* 5 *July* 1983)

Abstract—A numerical study is presented for the laminar flow and heat transfer in tubes with internal circumferential fins. The presence of the fins gives rise to a recirculating flow in the space between two successive fins. Computations are performed for the periodic fully developed flow, in which the velocity field repeats itself in successive inter-fin regions. Although the recirculating flow aids mixing and tends to increase the heat transfer, the obstruction provided by the fins causes the main throughflow to move away from the tube wall. The net effect is that, for fluids like air, there is actually a *decrease* in heat transfer for the finned tube. Only for high-Prandtl number fluids like water can some increase in heat transfer be achieved. The results are presented for a range of Reynolds numbers and for various values of the geometrical parameters such as the fin height and fin spacing. Streamline patterns are given for some typical cases to provide an insight into the heat transfer behavior.

NOMENCLATURE

c_p	specific heat at constant pressure
D	diameter of the tube, Fig. 1
f	friction factor, equation (8)
H	fin height, Fig. 1
$\bar{h}$	average heat transfer coefficient, equation (12)
k	thermal conductivity of the fluid
$\overline{Nu}$	overall Nusselt number, equation (11)
P	pitch of the fins, Fig. 1
Pr	Prandtl number
p	pressure
p^*	incremental pressure, equation (1)
Q	heat transfer rate per module
Q_{fin}	heat transfer rate from one fin
Re	Reynolds number, equation (10)
r	radial coordinate, Fig. 1
T	temperature
T^*	incremental temperature, equation (5)
T_b	bulk temperature, equation (13)
T_w	local wall temperature
$T_{w,0}$	wall temperature at $x = 0$, equation (6)
u	axial velocity
$\bar{u}$	cross-sectional average of u
v	radial velocity
x	axial coordinate, Fig. 1.

Greek symbols

β	overall pressure gradient, equation (1)
γ	axial gradient of T_w, equation (6)
μ	dynamic viscosity of the fluid
ρ	density of the fluid.

INTRODUCTION

AMONG the various heat transfer augmentation devices, the circular tube with internal fins is quite common. Normally, *radial* internal fins are used. The corresponding problem in both laminar and turbulent flows has received considerable attention. The present paper is concerned with laminar flow and heat transfer in circular tubes that contain *circumferential* internal fins. The geometry under consideration is shown in Fig. 1. The circumferential fins can be thought of as ring inserts or transverse ribs placed at regular intervals along the tube. Alternatively, periodic indentations of the tube wall lead to a somewhat similar geometry. Furthermore, it is possible to place twisted or helical fins inside tubes. When these are very tightly twisted, they resemble the circumferential fins. The resulting flow and heat transfer are expected to be similar except that the swirl imparted to the flow by twisted fins is absent in the circumferential-fin situation.

In the present study, it will be shown that, in *laminar* flow, the presence of the fins often *decreases* the heat transfer coefficient rather than augmenting it. On the other hand, heat transfer augmentation in *turbulent* flow by the use of ring inserts or rib roughness is well established. It is, therefore, important to note that the present paper pertains to laminar flow. In turbulent flow, the ribs act as turbulence promoters and periodically interrupt the formation of the laminar sublayer on the tube wall. There are no corresponding mechanisms at work when the flow is wholly laminar.

The need for heat transfer augmentation is actually greater in the laminar tube flow, since the smooth tube performs rather poorly under laminar flow conditions. When the flow must be laminar because of small dimensions, low flow rates, or highly viscous fluids, configurations are needed to enhance the rate of heat transfer. The purpose of this paper is to examine the influence of circumferential internal fins on the laminar flow and heat transfer in a tube.

In the configuration shown in Fig. 1, the fins have a height H and they are placed uniformly at a pitch P. In such a tube, the flow attains, after the initial entrance region, a *periodic* fully developed character, so that the

† Present address: Technology Advancement Division, Control Data Corporation, Minneapolis, MN 55440, U.S.A.

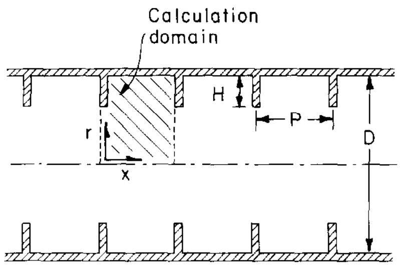

Fig. 1. Geometry of the problem.

flow field repeats itself in an identical fashion in successive geometrical modules formed by the presence of the fins. A calculation method has been developed in ref. [2] which can directly be used to compute the flow and heat transfer characteristics of the typical module shown in Fig. 1 without the need for the entrance-region calculation. For design purposes, the results for the typical module in the periodic fully developed region are often sufficient, since for tubes containing a large number of fins the somewhat different behavior of the entrance region becomes unimportant.

The present study provides numerical solutions for the typical module shown in Fig. 1. Computations are performed for different values of the Reynolds number and of the geometrical parameters H/D and P/H. The influence of the fin thickness on the flow field is ignored. The heat transfer results are obtained for three values of the Prandtl number, namely $Pr = 0.7$, 2.5, and 5. The values of 0.7 and 5 correspond to air and water, respectively. The value 2.5 equals the Schmidt number for the sublimation of naphthalene in air; thus, for $Pr = 2.5$, the heat transfer results would be comparable to the mass transfer obtained by the naphthalene-sublimation technique.

MATHEMATICAL FORMULATION

In the periodic fully developed flow to be analyzed, the fluid properties will be regarded as constant. As a consequence, the velocity field can be determined without simultaneously solving for the temperature field. Once the solution for the flow field is obtained, it can then be used in the subsequent solution of the temperature field.

For the typical computational module shown in Fig. 1, the flow is regarded as axisymmetrical, i.e. all variables depend only on x and r.

The velocity field

Because of the periodic nature of the flow, the pressure p can be expressed, as pointed out in ref. [2], by

$$p(x,r) = -\beta x + p^*(x,r), \tag{1}$$

where β is a constant and the function $p^*(x,r)$ identically repeats itself from module to module. The term βx represents the general decrease in pressure in the axial direction; βP gives the pressure drop over one module of axial length P. The quantity p^* indicates the local departure of pressure from the linear decay given by $-\beta x$.

The equations of motion for the flow can be written as

$$\frac{\partial u}{\partial x} + \frac{1}{r}\frac{\partial (rv)}{\partial r} = 0, \tag{2}$$

$$\rho u \frac{\partial u}{\partial x} + \rho v \frac{\partial u}{\partial r} = \beta - \frac{\partial p^*}{\partial x} + \mu \left[\frac{\partial^2 u}{\partial x^2} + \frac{1}{r}\frac{\partial}{\partial r}\left(r \frac{\partial u}{\partial r} \right) \right], \tag{3}$$

$$\rho u \frac{\partial v}{\partial x} + \rho v \frac{\partial v}{\partial r} = -\frac{\partial p^*}{\partial r} + \mu \left[\frac{\partial^2 v}{\partial x^2} + \frac{1}{r}\frac{\partial}{\partial r}\left(r \frac{\partial v}{\partial r} \right) - \frac{v}{r^2} \right]. \tag{4}$$

The boundary conditions for these equations are provided by the no-slip requirement on the tube wall and fin surfaces, by the symmetry conditions at the axis, and by the periodic behavior at the upstream and downstream faces of the module.

In a periodic fully developed flow, the boundary conditions do not involve a specified inflow rate. The actual flow rate is determined by the pressure gradient β, which must be specified to obtain a solution of equations (2)–(4). Thus, for a given pressure drop per module, the equations can be solved to yield a flow rate. When the equations and their boundary conditions are expressed in dimensionless form, they contain the geometrical parameters H/D and P/H and the pressure-gradient parameter $\rho\beta D^3/\mu^2$. From the resulting solution, the Reynolds number Re $(= \rho\bar{u}D/\mu)$ of the tube flow can be obtained. Thus, for a given geometry, there is a one-to-one correspondence between the pressure-gradient parameter and the resulting Reynolds number. In a numerical computation, it is possible to iteratively adjust the pressure gradient so that the converged solution corresponds to any desired value of the Reynolds number. From this reasoning, it is possible and convenient to consider that the velocity field in the module under consideration is determined by H/D, P/H, and Re.

The temperature field

A periodic regime can be identified for the temperature field only under certain thermal boundary conditions. The boundary condition employed here is one in which the temperature T_w of the tube wall varies linearly with the axial distance x. This condition is encountered in a counter-flow heat exchanger when the capacity flow rates of the two fluids are equal. The fluid temperature T can then be written as

$$T(x,r) = T_w(x) + T^*(x,r), \tag{5}$$

where $T_w(x)$ can be expressed as

$$T_w(x) = T_{w,0} + \gamma x. \tag{6}$$

The constant γ is the axial gradient of the wall temperature. The local departure of T from the wall temperature T_w is given by $T^*(x,r)$, which varies in a periodic manner from module to module.

The energy equation with T^* as the dependent variable can now be written as

$$\rho c_p\left(u\frac{\partial T^*}{\partial x}+v\frac{\partial T^*}{\partial r}\right)$$
$$=-\rho c_p u\gamma+k\left[\frac{\partial^2 T^*}{\partial x^2}+\frac{1}{r}\frac{\partial}{\partial r}\left(r\frac{\partial T^*}{\partial r}\right)\right]. \quad (7)$$

The temperature at the root of each fin would equal the value of T_w there. However, what temperature variation would prevail over the height of the fin depends upon the relative conductivities of the fin and the fluid. Here it is assumed that the fin material has a sufficiently high conductivity so that each fin remains isothermal at its root temperature. For metal fins in laminar flow, this assumption is expected to be very satisfactory.

The boundary conditions for T^* are given by a zero value at the tube wall and on the fin surface, the symmetry behavior at the tube axis, and periodicity at the upstream and downstream faces of the module.

The constant γ can be given any nonzero value; it simply acts as a scaling factor for the temperature field. In other words, equation (7) can be made dimensionless with $T^*/(\gamma D)$ as the dependent variable. The dimensionless equation would contain the Prandtl number Pr as the parameter.

Method of solution

The calculation procedure for periodic fully developed flows has been described in ref. [2]. The same procedure was used in the present study. The chosen calculation domain is shown in Fig. 1; it includes the region occupied by the fins in addition to that filled by the fluid. Although it is intended to ignore the effect of fin thickness, the fins were represented in the computations by a very small but nonzero thickness. This region was treated by setting the viscosity and the thermal conductivity there to be very large numbers. Such treatment for embedding solid regions in a fluid has been described in ref. [3].

The computations were carried out for $H/D = 0.05$, 0.1, and 0.2; P/H was varied from 1 to about 100 or until a further increase did not influence the results very much; the Reynolds number was changed from 100 to 1000. As mentioned earlier, three values of the Prandtl number, namely 0.7, 2.5, and 5.0 were used for the heat transfer calculations.

The majority of the runs were performed on a 22 × 42 grid in the x–r coordinates. Nonuniform grid spacing was used to provide sufficient resolution of the critical areas in the velocity and temperature fields. Extensive testing was performed to determine the sensitivity of the solutions to grid fineness. This is reported in detail in ref. [4]. For most conditions, the results for the 22 × 42 grid were almost identical to those for a 32 × 62 grid. Only at $Re = 1000$ and $H/D = 0.2$, was the error in the reported Nusselt number judged to be 1.5%. In general, the reported results can be regarded as accurate to at least 1.5%; in many cases, the accuracy is significantly better.

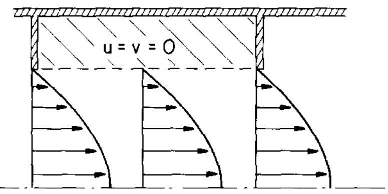

FIG. 2. Core flow model.

Core flow model

One way to judge the influence of the fins on heat transfer is to compare the resulting heat transfer coefficient with that for a finless tube. However, as will be shown later, the computed heat transfer coefficients for the finned tube turned out to be, in many cases, *lower* than those for the finless tube. To establish a lower bound for the heat transfer coefficient, another limiting situation was considered, which is here referred to as the core flow model.

The reason why the heat transfer coefficient may decrease for a finned tube is that the fins deflect the flow away from the tube wall. Thus, despite the extra area provided by the fins, the heat transfer on the tube wall and hence even the total heat transfer can diminish. In the core flow model, it is assumed that the fluid in the inter-fin space is completely stagnant, while the throughflow has a parabolic velocity profile in the central core of diameter $D-2H$. This distribution of the axial velocity u is shown in Fig. 2. The radial velocity v is assumed to be zero everywhere. With this known velocity field, equation (7) can be solved numerically to obtain the temperature field and the corresponding Nusselt number. As is well known for simple fully developed duct flows, the Nusselt number given by the core flow model would be independent of Re and Pr and would depend only on the geometry. (Strictly speaking, if conduction in the axial direction is included, the Nusselt number does depend on Re and Pr, or rather on the Peclet number $Re\,Pr$. But this is a weak dependence and was found to be negligible for the Peclet number encountered in this study.) The value of the Nusselt number given by the core flow model is expected to be similar to but lower than the actual Nusselt number based on the complex flow field caused by the fins. In such a flow field, there are recirculating motions in the inter-fin space which tend to increase the heat transfer. Therefore, the results from the core flow model are expected to serve as the lower bound for the actual results.

RESULTS AND DISCUSSION

The present numerical study produced extensive information in terms of the fields of velocity components, pressure, and temperature. Also, local and overall forces and heat transfer coefficients were

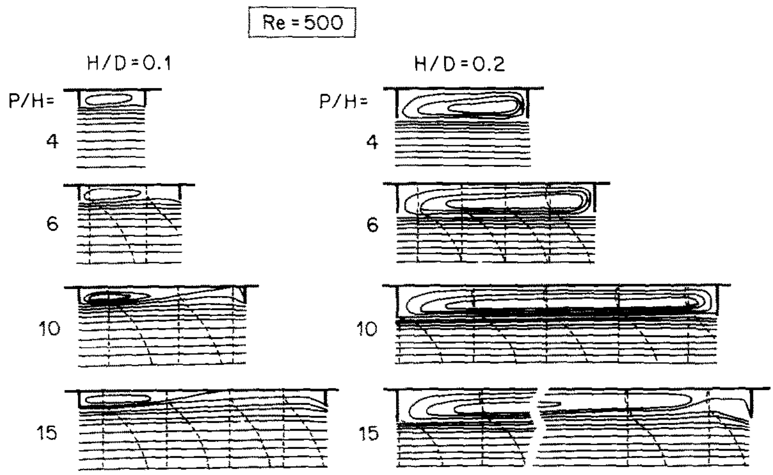

FIG. 3. Velocity fields for $Re = 500$.

calculated. A detailed presentation of the results can be found in ref. [4]. Here, only some important results are presented and discussed.

The velocity field

Figure 3 displays the velocity fields for $Re = 500$ and certain combinations of the geometrical parameters. Similar behavior was obtained for other values of the Reynolds number. The solid lines in the figure are the streamlines; the dashed curves indicate profiles of the axial velocity u.

For $H/D = 0.1$ the recirculation zone completely fills the inter-fin space for small values of P/H. At $P/H = 6$, there is a suggestion of reattachment of the flow to the tube wall. The reattachment is clearly visible for $P/H = 10$. As the value of P/H is further increased, the length of the recirculation zone remains unaltered and a greater portion of the tube wall experiences reattached flow. It is the presence of the recirculation zone and reattachment that influences heat transfer from the tube wall. For large P/H values, there is a very small recirculation zone on the upstream side of the fin.

The recirculation zones for $H/D = 0.2$ are more intense and their centers are shifted in the downstream direction. The tendency to reattach to the tube wall is delayed quite considerably; only at $P/H = 15$ is there some evidence of reattachment.

The axial velocity profiles shown by dashed lines indicate which of the simplified models would be appropriate in each case. When the inter-fin space is completely occupied by the recirculating flow, the axial velocity distribution is very similar to the one assumed in the core flow model. In the regions of attached flow, the profiles of u are akin to those for the fully developed flow in a finless tube. Thus, the heat transfer coefficients for the finned tube are expected to lie between those for the core flow model and ones for a simple tube flow, unless the recirculating flow has a very strong effect on heat transfer.

Friction factor

The complex flow fields generated by the presence of the fins influence the pressure gradient required to drive the flow. A dimensionless measure of the pressure gradient is the friction factor defined by

$$f = -(\mathrm{d}p/\mathrm{d}x)D/[(1/2)\rho\bar{u}^2]. \quad (8)$$

In equation (1), β was introduced as the magnitude of the overall pressure gradient for a module. The use of this value in equation (8) leads to

$$f\,Re = 2\beta D^2/(\mu\bar{u}), \quad (9)$$

where, in the product $f\,Re$, the Reynolds number Re is given by

$$Re = \rho\bar{u}D/\mu. \quad (10)$$

It is well known that the value of $f\,Re$ in a fully developed laminar tube flow is 64. For the finned tube, however, the values of $f\,Re$ are dependent on the Reynolds number, as will be seen shortly.

Figure 4 presents the variation of $f\,Re$ with P/H for three values of the Reynolds number and three fin heights. As P/H becomes very large, the fins become so infrequent that the behavior approaches that of the finless tubes. Thus, all curves have a tendency to be asymptotic to the finless tube value of 64, which is shown by a broken line and marked as $H/D = 0$. For the short fins ($H/D = 0.05$), the product $f\,Re$ has only a weak dependence on the Reynolds number since the geometry differs very little from that of the finless tube. The Reynolds number effect is seen to be strong for $H/D = 0.2$. In general, the $f\,Re$ values are large when the inter-fin space is completely filled by the recirculating fluid. When reattachment occurs, the tendency to approach the finless tube limit is established. The $f\,Re$ curves show a change of slope at the values of P/H where the flow fields indicate the start of reattachment.

In general, the very high values of $f\,Re$ represent the large penalty incurred in the use of the finned tubes. If

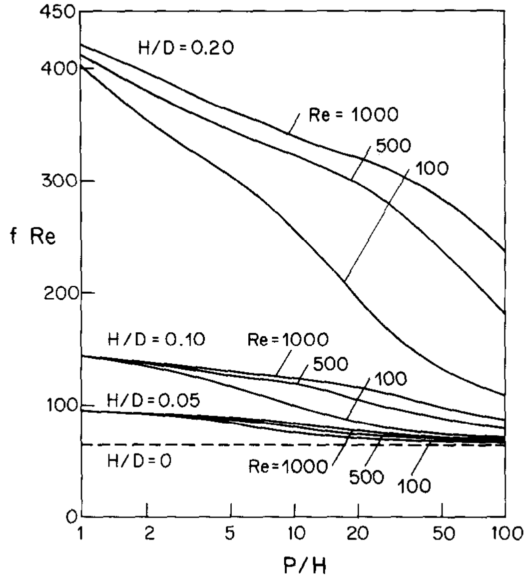

FIG. 4. Variation of the friction factor.

the resulting gain in heat transfer is not substantial, the large pressure drop should be regarded as unacceptable.

Overall heat transfer

The main objective of this study is to determine the influence of the fins on the heat transfer from the tube wall to the fluid. For his purpose, an overall Nusselt number is defined by

$$\overline{Nu} = \bar{h}D/k, \tag{11}$$

where the average heat transfer coefficient is calculated from

$$\bar{h} = Q/[\pi DP(T_w - T_b)]. \tag{12}$$

Here Q is the heat transfer rate to the fluid per module, πDP is the heat transfer area of the tube wall, and $T_w - T_b$ is the driving temperature difference. It should be noted that the area used in the definition of $\bar{h}$ does not include the extra area provided by the presence of the fins. Thus, $\bar{h}$ is based on the nominal area of a corresponding finless tube, rather than the actual surface area of the finned tube. An advantage of this definition is that it allows direct comparison of the $\overline{Nu}$ values for tubes with different H/D and P/H values. The magnitude of $\overline{Nu}$ reflects the combined effect of the increased area provided by the fins and the distortion of velocity and temperature fields caused by them.

The quantity T_b appearing in equation (12) is the bulk temperature of the fluid, which is defined as

$$T_b = \int_0^{D/2} T|u|r\, dr \bigg/ \int_0^{D/2} |u|r\, dr, \tag{13}$$

where the absolute values of u are used so that the integral is properly calculated in regions of reverse flow. Since both T_b and T_w depend on x, the difference $T_w - T_b$ is expected to be x-dependent. For the calculation of $\bar{h}$ from equation (12), the value of $T_w - T_b$ at $x = P/2$, i.e. at a location midway between two successive fins, was used. However, it was observed that the variation of $T_w - T_b$ with x was rather mild so that the use of different locations for the evaluation of $T_w - T_b$ would not have significantly affected the reported values of $\overline{Nu}$.

The quantity Q can be directly related to the temperature gradient γ introduced in equation (6) via an overall energy balance for the module. Thus

$$Q = (\rho\bar{u})(\pi D^2/4)c_p\gamma P, \tag{14}$$

where γP stands for the rise of the bulk temperature over one module (which equals the rise of the wall temperature per module in the periodic fully developed region).

In the case of a finless tube, the difference $T_w - T_b$ becomes invariant with x, and $\overline{Nu}$ equals the well-established value 4.364 for thermally developed heat transfer in a circular tube with a linearly rising wall temperature. Incidentally, in the absence of the fins, this boundary condition is identical to the uniform-heat-flux condition at the tube wall.

The values of $\overline{Nu}$ for all the cases studied are plotted in Figs. 5–7 for $H/D = 0.05$, 0.1, and 0.2, respectively. Each figure shows the variation of $\overline{Nu}$ with P/H for different Prandtl and Reynolds numbers. Also plotted are the curves for the results from the core flow model and a broken line for $\overline{Nu} = 4.364$, which is the value for a tube without fins.

Figure 5 shows the results for the small fin height, $H/D = 0.05$. For the most part, the $\overline{Nu}$ values are less than those for the finless tube. At $Re = 100$, since the recirculation is rather weak, the results depend little on

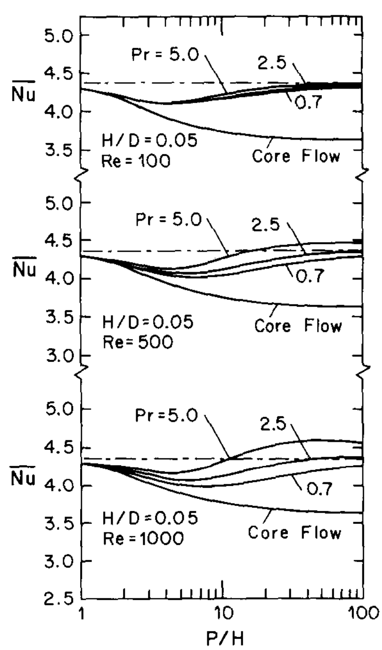

FIG. 5. Overall Nusselt number for $H/D = 0.05$.

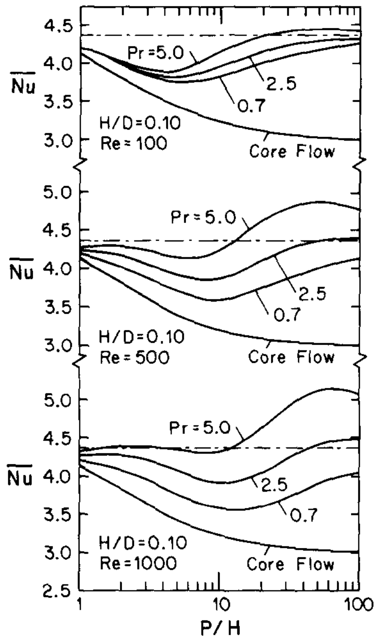

FIG. 6. Overall Nusselt number for $H/D = 0.1$.

the Prandtl number, with the increase of the Reynolds number, the recirculating flow gets stronger. As in other heat transfer augmentation devices, the recirculation has significant impact at high Prandtl numbers, for which the conduction heat transfer is small and any help from the convection process is very welcome. At low values of P/H, the inter-fin space is filled with low-velocity recirculating fluid. The flow condition is thus akin to the core flow model, which provides a good approximation of the behavior at low P/H. As P/H increases, the recirculating flow becomes stronger, but the extra area provided by the fins diminishes. As a result, the value of the Nusselt number, although better than the core-flow prediction, decreases and attains a minimum. The upturn in the $\overline{Nu}$ curves occurs as a result of the reattachment of the flow. Then at least a part of the tube wall is directly washed by the throughflow, and the $\overline{Nu}$ values return to the level appropriate for the finless tube. For $Pr = 5$, the benefit derived from recirculating flow is large enough to slightly exceed the finless-tube value of $\overline{Nu}$.

The same general trends, albeit in an enlarged form, are seen in Figs. 6 and 7. For higher H/D, the decrease of heat transfer area with P/H is faster; the recirculating flows are more intense; and the reattachment is delayed to larger values of P/H. After the reattachment, a peak in the $\overline{Nu}$ value is reached, after which further decrease in the heat transfer area causes a decline in $\overline{Nu}$.

In Fig. 7, at small values of P/H, $\overline{Nu}$ appears to increase with P/H. This behavior, which is also somewhat noticeable in Fig. 6, requires some comment. When H/D is large, the fins form a major proportion of the heat transfer area especially at small values of P/H. The strength of the recirculating flow increases with P/H. As a result, although the tube wall transfers less heat than its finless counterpart, the fins are washed by faster transverse flow. This leads to the increased $\overline{Nu}$ observed around $P/H = 2$.

Fin heat transfer

Since the overall results presented so far represent the total contribution of the fin and the tube wall, it is now instructive to consider the separate contribution of the fin to the total heat transfer. Figure 8 shows the ratio of Q_{fin}/Q as a function of P/H for $H/D = 0.1$ and $Re = 500$. This is presented here as it is typical of the behavior observed in other cases. Such diagrams for all the cases considered in Figs. 5–7 are available in ref. [4]. The quantity Q_{fin} is the heat transferred by one fin per module; Q represents the total heat transfer per

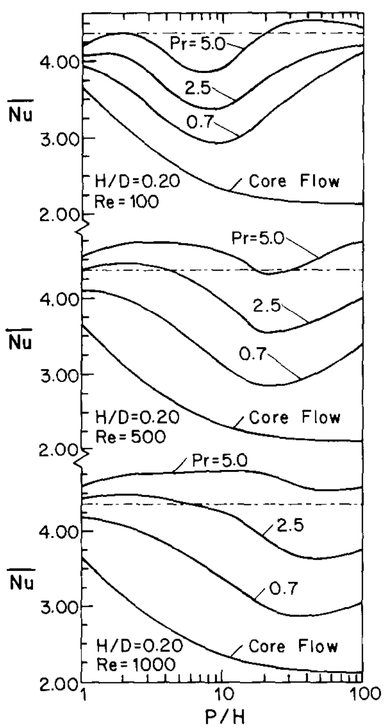

FIG. 7. Overall Nusselt number for $H/D = 0.2$.

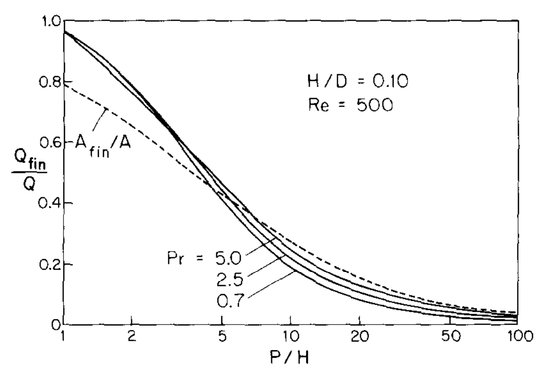

FIG. 8. Heat transfer contributed by the fin.

module. The dashed line represents the area ratio A_{fin}/A as a function of P/H. When the Q_{fin}/Q curve lies above the dashed line, the fin can be considered to transfer more heat than the tube wall on a unit area basis.

It can be seen from Fig. 8 that the relative effectiveness of the fin does not significantly depend on the Prandtl number. The convection process is expected to influence both the fin and the tube wall in almost equal manner. Until about a P/H of 5 or 6, the fin transfers more heat than the wall does on a unit area basis. Beyond $P/H = 6$, the wall becomes more active. As observed in Fig. 3, $P/H = 6$ corresponds to the geometry at which reattachment begins for $Re = 500$. Only for $P/H > 6$ does the tube wall begin to experience a direct impingement by the throughflow. This explains the crossover of the solid and dashed curves in Fig. 8.

CONCLUDING REMARKS

This study has presented numerical results for the laminar flow and heat transfer in circular tubes with circumferential internal fins. The outcome that was initially surprising to the present authors is that a finned duct does not always increase heat transfer. Despite the increased area provided by the fins, the distortion of the flow that the fins cause can substantially diminish the heat transfer from the duct wall and thus lower the overall heat transfer. The circumferential fins were found to augment heat transfer only for a Prandtl number of 5. For lower Prandtl numbers, a reduction in heat transfer was obtained.

It may be noted that, in this analysis, the fins were assumed to be made of a high-conductivity material. The heat transfer would be even lower if finite conductivity of the fin material and imperfect contact between the fins and the tube wall were taken into account.

An insight into the overall heat transfer behavior has been obtained through the examination of the flow fields. Also a simplified flow model of the situation has been developed to simulate the extreme flow-obstructing effect of the fins. The results from this model serve as the lower limit of the predicted heat transfer.

Acknowledgement—This research was performed under the auspices of a grant from the National Science Foundation.

REFERENCES

1. R. L. Webb, Turbulent heat transfer in tubes using two-dimensional roughness, including the effect of Prandtl number, Ph.D. thesis, University of Minnesota (1969).
2. S. V. Patankar, C. H. Liu and E. M. Sparrow, Fully developed flow and heat transfer in ducts having streamwise-periodic variation of cross-sectional area, *Am. Soc. Mech. Engrs*, Series C, *J. Heat Transfer* **99**, 180–186 (1977).
3. S. V. Patankar, A numerical method for conduction in composite materials, flow in irregular geometries, and conjugate heat transfer, *Proc. 6th Int. Heat Transfer Conf.*, Toronto, Vol. 3, p. 297 (1978).
4. G. J. Rowley, Heat transfer and fluid analysis of internal, circumferentially finned tubes in laminar flow, M.S. thesis, University of Minnesota (1981).

ANALYSE DE L'ECOULEMENT LAMINAIRE ET DU TRANSFERT THERMIQUE DANS DES TUBES AVEC DES AILETTES PERIPHERIQUES INTERNES

Résumé—On présente une étude numérique de l'écoulement laminaire et du transfert thermique dans des tubes avec des ailettes périphériques internes. La présence des ailettes donne lieu à un écoulement de recirculation dans l'espace entre deux ailettes successives. Des calculs pour l'écoulement périodique complètement établi, dans lequel le champ de vitesse se reproduit dans les régions successives entre ailettes. Bien que l'écoulement de recirculation aide le mélange et tende à augmenter le transfert thermique, l'obstruction par les ailettes éloigne de la paroi l'écoulement. L'effet net est que, pour des fluides comme l'air, il se produit une *décroissance* du transfert pour le tube aileté. Seul pour les fluides à grand nombre de Prandtl comme l'eau, on obtient un accroissement de transfert thermique. Les résultats sont présentés pour un domaine de nombre de Reynolds et pour différentes valeurs des paramètres géométriques comme la hauteur et l'espacement des ailettes. Les configurations d'écoulement sont données pour quelques cas typiques pour éclairer le comportement thermique.

UNTERSUCHUNG DER LAMINAREN STRÖMUNG UND DES WÄRMEÜBERGANGS IN EINEM ROHR MIT INNEREN KREISRIPPEN

Zusammenfassung—Es wird eine numerische Untersuchung der laminaren Strömung und des Wärmeübergangs in einem Rohr mit Kreisrippen am inneren Umfang beschrieben. Durch das Vorhandensein der Rippen wird eine Rezirkulationsströmung im Gebiet zwischen zwei aufeinanderfolgenden Rippen verursacht. Für die periodische, voll ausgebildete Strömung, bei der sich das Geschwindigkeitsfeld in aufeinanderfolgenden Rippenzwischenräumen ständig wiederholt, wurden Berechnungen durchgeführt. Obgleich die Rezirkulationsströmung die Durchmischung fördert und damit der Wärmeübergang ansteigt, bewirken die Rippen als Strömungshindernisse, daß sich der Hauptstrom von der Rohrwand entfernt. Die effektive Wirkung der Innenberippung des Rohres ist, daß der Wärmeübergang für Fluide, wie z. B. Luft, abnimmt. Nur für Fluide mit großen Prandtl-Zahlen, wie z. B. Wasser, kann ein geringer Anstieg des Wärmeübergangs erzielt werden. Die Ergebnisse sind für einen Bereich von Reynolds-Zahlen und für verschiedene Werte der geometrischen Parameter wie Rippenhöhe und Rippenabstand angegeben. Um einen Einblick in das Wärmeübergangsverhalten zu geben, wurde der Verlauf der Stromlinien für einige typische Fälle dargestellt.

АНАЛИЗ ЛАМИНАРНОГО ТЕЧЕНИЯ И ТЕПЛОПЕРЕНОСА В ТРУБАХ С РАСПОЛОЖЕННЫМИ ВНУТРИ ПО ОКРУЖНОСТИ РЕБРАМИ

Аннотация—Представлено численное исследование ламинарного течения и теплопереноса в трубах с расположенными внутри по окружности ребрами. Такая конфигурация вызывает рециркуляционные потоки в пространстве между двумя соседними ребрами. Выполнены расчеты для периодического полностью развитого течения, при котором поле скорости повторяется в последовательно расположенными между ребрами областях. Несмотря на то, что рециркуляция способствует перемешиванию и интенсификации теплопереноса, оказываемое ребрами сопротивление основному потоку вызывает его оттеснение от стенки трубы. В результате в случае течения газов типа воздух происходит снижение теплопереноса в оребренной трубе. Только при течении жидкостей, характеризующихся большим числом Прандтля, как например вода, можно получить некоторое увеличение интенсивности теплопереноса. Представлены результаты для ряда чисел Рейнольдса и различных значений таких геометрических параметров, как высота ребер и расстояние между ними. Для некоторых типичных случаев даны картины линий тока для лучшего понимания процесса теплопереноса.